

CRes User Guide

LEIGHTON M. WATSON
Stanford University
leightonwatson@stanford.edu

March 27, 2019

I. INTRODUCTION

CRes (Crater Resonance) is a one-dimensional (1D) numerical method for solving the linear acoustic wave equation within a volcanic crater. For a specified crater geometry and excitation source at the base of the crater, **CRes** computes the velocity and pressure at the crater outlet and can propagate the signal to an infrasound receiver some distance from the outlet. The linear acoustic wave equation is written in terms of two first-order differential equations for pressure and acoustic flow and is solved by **CRes** using a finite-difference frequency-domain method. **CRes** is written in MATLAB and runs efficiently on a standard desktop/laptop computer. For more details and examples of the application of **CRes** see:

- Watson, L. M., Dunham, E. M., and Johnson, J. B. Simulation and inversion of harmonic infrasound from open-vent volcanoes using an efficient quasi-1D crater model, *Journal of Volcanology and Geothermal Research*, submitted 28 Dec 2018, revised 19 Mar 2019.
- Johnson, J. B., Watson, L. M., Palma, J. L., Dunham, E. M., and Anderson, J. F. (2018) Forecasting the eruption of an open-vent volcano using resonant infrasound tones, *Geophysical Research Letters*, 45, <https://doi.org/10.1002/2017GL076506>.

II. DIRECTORY

- **demo** - script files for demonstration
 - `exampleX.m` - example script files
 - `Johnson2018.mat` - example crater geometry from Johnson et al. (2018)
 - `Richardson2014.mat` - example crater geometry from Richardson et al. (2014)
- **doc** - documentation including user guide and license file
- **source/SBPoperators** - function files associated with numerical implementation
- **source/resonance** - function files for **CRes**
 - `resonance1d.m` - main code
 - `problemParameters` - specifies model parameters
 - `pressurePerturbation.m` - computes pressure perturbation (infrasound signal) at a distance away from the crater
 - `flanged_opening.m` - treatment of open end of crater
 - `resPeakProps.m` - computes resonant frequency and quality factor of spectral peaks
 - `sourceFunction.m` - specifies source function (Gaussian or Brune)

CRes is freely available online at <https://github.com/leighton-watson/CRes> and is distributed under the MIT license.

III. MODEL DESCRIPTION

Here, I provide an overview of **CRes**. For more details see Watson et al., (2019). **CRes** assumes linear wave propagation, which enables the infrasound signal, Δp , observed at a distance, r , from the crater outlet to be written as:

$$\Delta p(t, r) = T(t, r) * s(t) \quad (1)$$

where T is the acoustic response function, which depends on the crater and atmospheric properties, that describes the theoretical infrasound signal generated by an impulsive excitation at the base of the crater, and $s(t)$ is the finite-duration source at the base of the crater. The source expressed as a volumetric flow rate of air within the crater being push upwards, or pulled downwards, by the source process (m^3/s). **CRes** is written in the frequency domain where the time-domain convolution is replaced by multiplication:

$$\Delta p(\omega, r) = T(\omega, r)s(\omega), \quad (2)$$

where ω is the angular frequency.

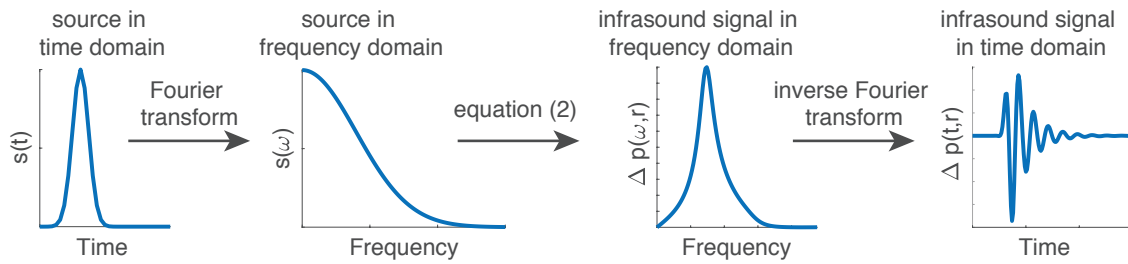


Figure 1: The modeling workflow is to start with a specified source function, $s(t)$, and take the Fourier transform to get $s(\omega)$. The infrasound signal in the frequency domain, $\Delta p(\omega, r)$, is calculated by equation 2 and the inverse Fourier transform is used to obtain the infrasound signal in the time domain, $\Delta p(t, r)$.

The acoustic response function, T , is divided into 1.) the crater acoustic response function, C , which describes wave propagation and resonant modes inside the volcanic crater, and 2.) the atmospheric response function, P , which describes acoustic radiation from the crater to the infrasound station.

i. Crater Acoustic Response Function

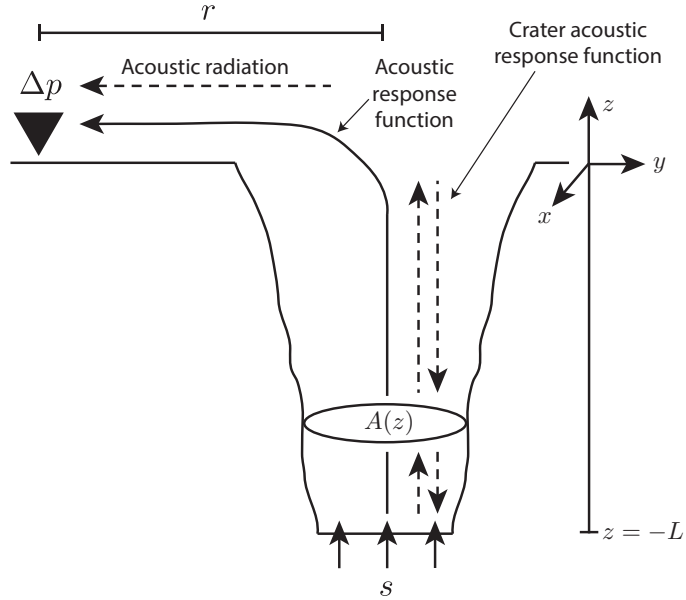
This section describes how to calculate the crater acoustic response function, C . The crater is modeled as quasi-one-dimensional (allowing for changes in cross-sectional area with depth) and axisymmetric. Acoustic waves inside the crater are described by linear acoustics written as a system of first-order partial differential equations:

$$\frac{\partial U}{\partial t} + \frac{A}{\rho} \frac{\partial p}{\partial z} = 0, \quad (3)$$

$$\frac{\partial p}{\partial t} + \frac{K}{A} \frac{\partial U}{\partial z} = 0, \quad (4)$$

where p is the pressure, $U = vA$ is the acoustic flow where A is the cross-sectional area, which can vary as a function of depth, and v is the vertical particle velocity. The air inside the crater is

Figure 2: Schematic of model. The infrasound signal, Δp , observed at a distance r from the crater is related to the excitation source at the base of the crater, s , by the acoustic response function, T , which includes the crater acoustic response function that describes wave propagation inside the crater and associated resonant modes, and the atmosphere response function, which describes acoustic radiation from the crater outlet to the receiver.



described as an ideal gas with ambient density, ρ , and fluid bulk modulus, K , which is proportional to the ambient pressure for an ideal gas. Density and pressure are related by the ideal gas equation of state:

$$p = \rho RT, \quad (5)$$

where R is the specific gas constant and T is the temperature, not to be confused with response function T in equations (1) and (2). The speed of sound is

$$c = \sqrt{\gamma RT}, \quad (6)$$

where γ is the ratio of specific heats ($\gamma = 1.4$ for diatomic gases such as air).

The governing equations are solved in the frequency domain and can be written as a system of first-order ordinary differential equations:

$$i\omega U + \frac{A}{\rho} \frac{\partial p}{\partial z} = 0, \quad (7)$$

$$i\omega p + \frac{K}{A} \frac{\partial U}{\partial z} = 0. \quad (8)$$

The model requires two boundary conditions, one at the bottom of the crater and one at the crater outlet. At the bottom, $z = -L$, of the crater the acoustic flow is specified as the source-time function:

$$U(t, -L) = s(t) = \iint_{A(L)} v(x, y, t) \, dx \, dy. \quad (9)$$

At the crater outlet, $z = 0$, the pressure and acoustic flow are related by the terminating impedance, Z_T (Rossing and Fletcher, 2004):

$$\frac{p(\omega, 0)}{U(\omega, 0)} = Z_T(\omega). \quad (10)$$

A constant pressure boundary condition could be applied at the outlet. However, this results in perfect reflection of acoustic waves. In order to allow acoustic waves to escape

into the atmosphere and be recorded as infrasound, a more accurate description of the outlet is required. Here, a flanged opening is assumed (Olson, 1957; Kinsler et al., 2000; Rossing and Fletcher, 2004) and the terminating impedance is given by (Rossing and Fletcher, 2004)

$$Z_T = R + iX, \quad (11)$$

where i indicates the imaginary unit, R is the acoustic resistance

$$R = Z_a \left[\frac{(ka)^2}{2} - \frac{(ka)^4}{2^2 \cdot 3} + \frac{(ka)^6}{2^2 \cdot 3^2 \cdot 4} - \dots \right], \quad (12)$$

and X is the acoustic reactance

$$X = \frac{Z_a}{\pi(ka)^2} \left[\frac{(2ka)^3}{3} - \frac{(2ka)^5}{3^2 \cdot 5} + \frac{(2ka)^7}{3^2 \cdot 5^2 \cdot 7} - \dots \right], \quad (13)$$

with k the wavenumber, a the crater radius at the outlet and $Z_a = \rho_a c_a / A(0)$ where ρ_a and c_a are the density and speed of sound in the atmosphere, respectively, and $A(0)$ is the cross-sectional area of the crater outlet.

ii. Atmospheric Response Function

This section describes how to calculate the atmospheric response function, P . Propagation of the infrasound signal from the crater outlet to the receiver is described as axisymmetric radiation from a baffled piston embedded in an infinite plane (Rossing and Fletcher, 2004):

$$\Delta p(\omega, r) = i\omega \exp(-ikr) \frac{\rho_a a^2}{2r} \left[\frac{2J_1(ka \sin \theta)}{ka \sin \theta} \right] \frac{U(\omega, 0)}{\pi a^2}, \quad (14)$$

where J_1 is a Bessel function of order one, θ is the angle between the negative z -axis and the receiver (e.g., $\theta = \pi/2$ for a receiver located on the plane perpendicular to crater orientation), ρ_a is the density of the atmosphere, and a is the crater radius at the outlet. The baffled piston model reduces to the monopole source description (e.g., Woulff and McGetchin, 1976; Johnson and Miller, 2014) for radiation in a half-space in the low frequency limit when $ka \ll 1$,

$$\Delta p(\omega, r) = i\omega \exp(-ikr) \frac{\rho_a a^2}{2r} \frac{U(\omega, 0)}{\pi a^2}. \quad (15)$$

IV. NUMERICAL IMPLEMENTATION

Equations 7 and 8 are solved using a summation-by-parts finite-difference discretization scheme (Del Rey Fernández et al., 2014; Svärd and Nordström, 2014), which is discussed in this section.

The domain ($-L \leq z \leq 0$) is discretized into $N + 1$ evenly spaced grid points, z_i , $i = 0, 1, 2, \dots, N$ where $z_0 = -L$ is at the base of the crater where the source is located and $z_N = 0$ is at the top of the crater. A field such as $p(z, t)$ is approximated at the grid points with the grid values stored in a vector $\mathbf{p}(t)$ with components $p_i(t) \approx p(z_i, t)$. The spatial derivatives are approximated using a summation-by-parts (SBP) differentiation matrix, \mathbf{D} , such that the vector $\mathbf{D}\mathbf{p}$ contains approximations to $\partial p / \partial z$ at the grid points (Karlstrom and Dunham, 2016). The discrete equations are

$$i\omega \mathbf{U} + \frac{A}{\rho_{\text{amb}}} \mathbf{D}\mathbf{p} = -\theta_1(U_0 - \hat{U}_0)\mathbf{e}_0 - \theta_2(U_N - \hat{U}_N)\mathbf{e}_N, \quad (16)$$

$$i\omega \mathbf{p} + \frac{K}{A} \mathbf{D}\mathbf{U} = -\theta_3(p_0 - \hat{p}_0)\mathbf{e}_0 - \theta_4(p_N - \hat{p}_N)\mathbf{e}_N, \quad (17)$$

where the terms on the right are the implementation of the boundary conditions in the SAT framework. Scalars $\theta_1 - \theta_4$ are penalty parameters that are chosen to ensure a stable numerical discretization (Kozdon et al., 2012):

$$\theta_1 = \theta_3 = \frac{c}{H_{00}}, \quad (18)$$

$$\theta_2 = \theta_4 = \frac{c}{H_{NN}}, \quad (19)$$

where H is a symmetric positive definite matrix such that $D = H^{-1}Q$ where Q is an almost skew symmetric matrix with the property that $Q^T + Q = \text{diag}[-1 \ 0 \ \dots \ 0 \ 1]$ (Karlstrom and Dunham, 2016).

The variables with a circumflex, $\hat{U}_0, \hat{U}_N, \hat{p}_0, \hat{p}_N$, are the target values for acoustic flow and pressure at the boundary points while U_0, U_N, p_0 and p_N are the known grid values. The target values are chosen to satisfy the desired boundary conditions exactly while preserving the characteristic variable carrying information from the interior of the domain to the boundary. The vectors $e_0 = [1 \ 0 \ \dots \ 0]^T$ and $e_N = [0 \ \dots \ 0 \ 1]^T$ isolate the effect of the penalty terms to the boundary points (Karlstrom and Dunham, 2016).

The characteristic variables that carry information from the interior of the domain to the boundaries are

$$p_0 - Z_0 U_0 = \hat{p}_0 - Z_0 \hat{U}_0, \quad (20)$$

$$p_N + Z_N U_N = \hat{p}_N + Z_N \hat{U}_N, \quad (21)$$

where $Z = \rho c / A$ is the acoustic impedance.

The velocity is specified at the base of the crater, $\hat{U}_0 = \text{specified}$. Rearranging equation 20 gives

$$\hat{p}_0 = p_0 + Z_0(\hat{U}_0 - U_0). \quad (22)$$

At the crater outlet, the pressure is related to the acoustic flow by the terminating impedance, Z_T :

$$\hat{p}_N = Z_T \hat{U}_N. \quad (23)$$

The terminating impedance is calculated using a flanged opening approximation (equation 11; Kinsler et al., 2000; Rossing and Fletcher, 2004). Substituting equation 23 into equation 21 gives the outlet boundary conditions:

$$\hat{U}_N = \frac{p_N + Z_N U_N}{Z_T + Z_N}, \quad (24)$$

$$\hat{p}_N = Z_T \left(\frac{p_N + Z_N U_N}{Z_T + Z_N} \right). \quad (25)$$

V. EXAMPLES

For demonstration purposes, two example script files are included that simulate crater acoustic resonance at Villarrica volcano. `example1.m` computes the resonant modes of Villarrica's crater for a single depth while `example2.m` shows how to compute the resonant frequency and quality factor as a function of the position of the lava lake within the crater. The crater geometry has been previously calculated from visual observations using structure-from-motion (Johnson et al., 2018) and is saved as `Johnson2018.mat`.

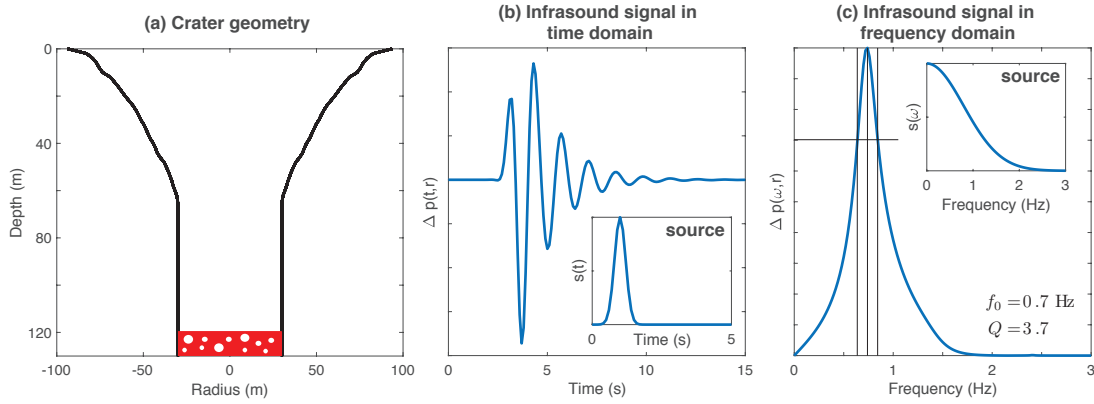


Figure 3: Outputs from `example1.m` showing (a) crater geometry with lava lake at 120 m below the crater rim, (b) infrasound signal in the time domain and (c) in the frequency domain. Insets show the source (volumetric flow rate at base of crater/surface of lava lake).

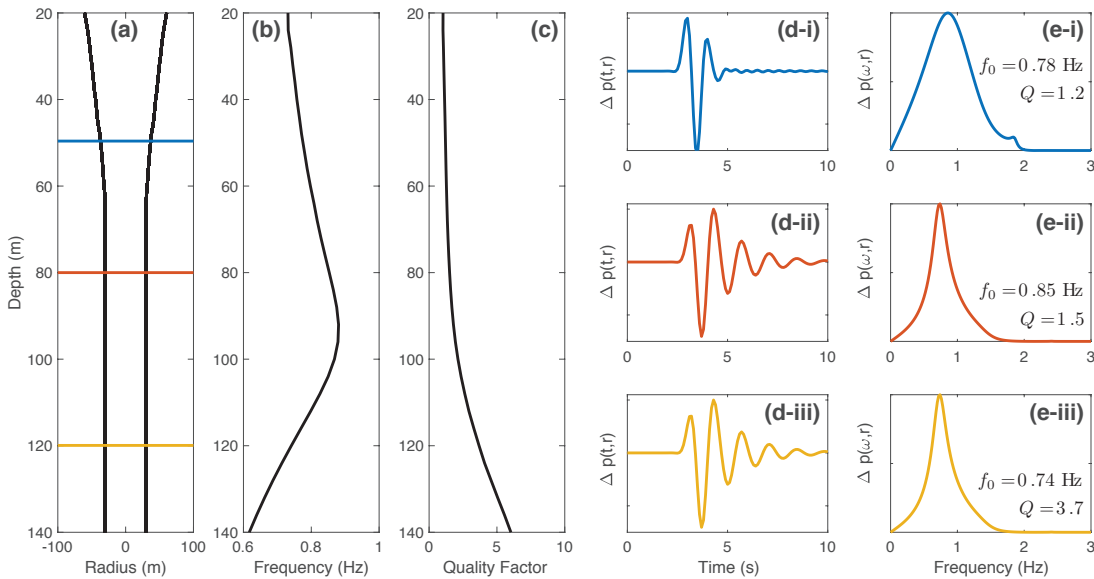


Figure 4: Outputs from `example2.m` showing simulated infrasound signal as a function of depth. (a) Crater geometry, (b) Resonant frequency and (c) quality factor as a function of depth. Infrasound signal in the (d) time and (e) frequency domains for crater depths of (i) 50 m, (ii) 80 m, and (iii) 120 m. Acoustic waves are excited by a Gaussian pulse with $\sigma = 0.2$ s, the same source as for `example1.m`.

VI. CRes FUNCTIONS

This section contains the details and syntax of the different function files used by **CRes**:

- i resonanceld
- ii flanged_opening
- iii problemParameters
- iv pressurePerturbation
- v resPeakProps
- vi sourceFunction

i. resonanceld

```
function output = resonanceld(geometry, depth, freq, Nf, style, order, M)
% computes the acoustic response function for an axisymmetric crater
%
% INPUT
% geometry = vector containing the depth (:,1) and radius (:,2) of the crater starting
%             from the deepest depth
% depth = depth of base of crater
% freq = maximum and minimum frequency of interest
% Nf = number of frequency samples
% style = sound radiation description ('baffled piston' or 'monopole')
% order = internal order of accuracy
% M = model parameters
%
% OUTPUT
% solver outputs are saved into the structure output
% output.geometry = crater geometry in the same format as input geometry
% output.depth = depth of base of crater
% output.f = frequency vector
% output.T = transfer function
% output.pOutlet = outlet pressure transfer function
% output.vOutlet = outlet velocity transfer function
% output.P = far-field pressure perturbation transfer function
```

ii. problemParameters

This function defines the properties of crater and atmosphere and saves these parameters into a structure that can be accessed by the other functions.

```
function M = problemParameters()
% Store properties of atmosphere and crater in structure M
%
% INPUT
% No inputs
%
% OUTPUT
% M = structure containing properties of atmosphere and crater
% M.gamma = ratio of heat capacities
% M.r = distance from outlet to receiver
% M.R = specific gas constant
% M.TA = atmospheric temperature [C]
% M.rhoA = density of atmospheric air [kg/m^3]
```

```
% M.cA = sound of sound in atmosphere [m/s]
% M.TC = crater temperature [C]
% M.rhoC = density of air within crater [kg/m^3]
% M.cC = speed of sound within crater [m/s]
% M.pC = pressure inside crater [Pa]
```

iii. pressurePerturbation

`pressurePerturbation.m` takes the outputs of `resonance1d.m`, specifically the acoustic flow at the outlet, and computes the pressure perturbation at a specified distance from the crater outlet. Here, we include two possible axisymmetric acoustic radiation models:

1. Baffled piston (Rossing and Fletcher, 2004):

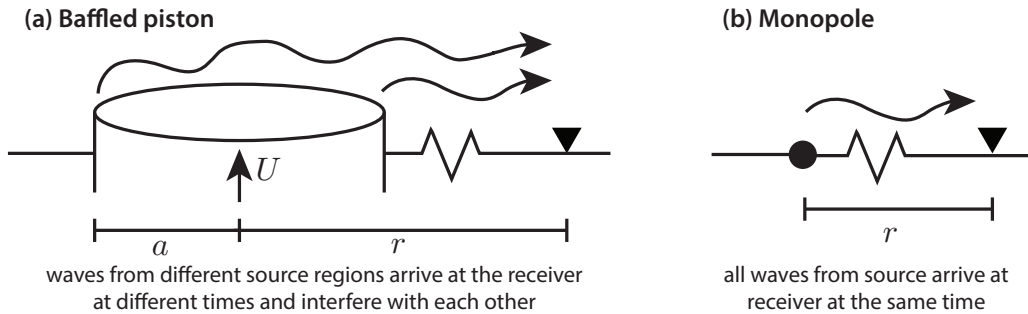
$$\Delta p(\omega, r) = i\omega \exp(-ikr) \frac{\rho_a a^2}{2r} \left[\frac{2J_1(ka \sin \theta)}{ka \sin \theta} \right] \frac{U(\omega, 0)}{\pi a^2}, \quad (26)$$

where $\Delta p(\omega, r)$ is the excess pressure at a distance r from the crater outlet, J_1 is a Bessel function of order one, θ is the angle between the negative z -axis and the receiver (e.g., $\theta = \pi/2$ for a receiver located on the plane perpendicular to crater orientation), ρ_a is the density of the atmosphere, a is the crater radius at the outlet, and $U(\omega, 0)$ is the acoustic flow at the crater outlet. The baffled piston model accounts for the finite dimension of the crater outlet.

2. Monopole (Woulff and McGetchin, 1976; Johnson and Miller, 2014):

$$\Delta p(\omega, r) = i\omega \exp(-ikr) \frac{\rho_a a^2}{2r} \frac{U(\omega, 0)}{\pi a^2}. \quad (27)$$

Note that the baffled piston model reduces to the monopole model in the low frequency limit when $ka \ll 1$.



It is noted that an alternative wave propagation code could be used to propagate the signal from the crater outlet to the infrasound receiver. For instance, if the surrounding topography outside of the crater is too complex to be approximated as axisymmetric then a 3D wave propagation code such as *infraFDTD* (Kim and Lees, 2011) could be used.

```
function P = pressurePerturbation(input, style, M)
% Computes pressure perturbation at specified distance from outlet
%
% INPUT
```



```
% input = output structure from resonanceld
% style = style of acoustic radiation. Options are "baffled piston" or "monopole"
% M = structure containing model parameters
%
% OUTPUT
% P = pressure perturbation in frequency domain at specified distance from outlet
```

iv. flanged_opening

```
function Z = flanged_opening(f,rho,c,a)
% computes terminating impedance of opening through rigid flange
%
% INPUT
% omega = angular frequency []
% rho = density of atmospheric air [kg/m^3]
% c = sound speed in atmosphere [m/s]
% a = radius of outlet [m]
%
% OUTLET
% Z = terminating impedance
```

v. resPeakProps

resPeakProps.m computes the resonant frequency and quality factor of the fundamental resonant mode of the provided amplitude spectra.

```
function [f0, Q] = resPeakProps(f,G)
% computes resonant frequency and quality factor of fundamental resonant mode.
%
% INPUT
% f = frequency vector
% G = amplitude spectra
%
% OUTPUT
% f0 = resonant frequency
% Q = quality factor
```

vi. sourceFunction

sourceFunction.m can be used to compute the excitation source in both time and frequency domains. Currently there are two possible source styles to choose from: 1.) Gaussian:

$$s(t) = S \exp\left(-\frac{1}{2} \frac{t^2}{\sigma^2}\right), \quad (28)$$

where S is the source amplitude and σ is the source width, and 2.) Brune

$$s(t) = StH(t) \exp\left(-\frac{t}{\sigma}\right), \quad (29)$$

where H is the Heaviside function. Alternatively, instead of using sourceFunction.m the user can define their own source function.

```
function [S,f,s,t] = sourceFunction(A,L,srcStyle,resParams)
% Compute source function in the time and frequency domains.
%
```

```
% INPUT
% A = source amplitude
% L = source width
% srcStyle = style of source mechanism ('Gauss' or 'Brune')
% resParams = parameters to ensure consistency with resonance1d simulation
%
% OUTPUT
% S = source function in frequency domain
% f = frequency vector
% s = source function in time domain
% t = time vector
```

REFERENCES

- Del Rey Fernández, D. C., Hicken, J. E., Zingg, D. W., 2014. Review of summation-by-parts operators with simultaneous approximation terms for the numerical solution of partial differential equations. *Computers and Fluids* 95, 171–196.
- Johnson, J. B., Miller, A. J. C., 2014. Application of the Monopole Source to Quantify Explosive Flux during Vulcanian Explosions at Sakurajima Volcano (Japan). *Seismological Research Letters* 85 (6).
- Johnson, J. B., Watson, L. M., Palma, J. L., Dunham, E. M., Anderson, J. F., 2018. Forecasting the eruption of an open-vent volcano using resonant infrasound tones. *Geophysical Research Letters*, 1–8.
- Karlstrom, L., Dunham, E. M., 2016. Excitation and resonance of acoustic-gravity waves in a column of stratified , bubbly magma. *Journal of Fluid Mechanics* 797, 431–470.
- Kim, K., Lees, J. M., 2011. Finite-difference time-domain modeling of transient infrasonic wavefields excited by volcanic explosions. *Geophysical Research Letters* 38 (6), 2–6.
- Kinsler, L. E., Frey, A. R., Coppers, A. B., Sanders, J. V., 2000. *Fundamentals of Acoustics*, 4th Edition. John Wiley and Sons, New York.
- Kozdon, J. E., Dunham, E. M., Nordström, J., 2012. Interaction of waves with frictional interfaces using summation-by-parts difference operators: Weak enforcement of nonlinear boundary conditions. *Journal of Scientific Computing* 50 (2), 341–367.
- Olson, H. F., 1957. *Acoustical engineering*. Van Nostrand Company, Princeton, New Jersey.
- Richardson, J. P., Waite, G. P., Palma, J. L., 2014. Varying seismic-acoustic properties of the fluctuating lava lake at Villarrica volcano, Chile. *Journal of Geophysical Research: Solid Earth*, 1–14.
- Rossing, T. D., Fletcher, N. H., 2004. *Principles of Vibration and Sound*, 2nd Edition. Vol. 1. Springer.
- Svärd, M., Nordström, J., 2014. Review of summation-by-parts schemes for initial-boundary-value-problems. *Journal of Computational Physics* 268, 17–38.
- Woulff, G., McGetchin, T. R., 1976. *Acoustic noise from volcanoes - Theory and experiment*.